Supporting information

Mechanochemical biomimetic mineralization of UiO-66-NH_2-immobilized cellulase for enhanced catalytic stability and efficiency

Xiaoyang Sun[1], Linyu Nian[1], Huimin Qi, Mengjun Wang, Dechun Huang, Chongjiang Cao*

Department of Food Quality and Safety/National R&D Center for Chinese Herbal Medicine Processing, College of Engineering, China Pharmaceutical University, Nanjing 211198, China

*Corresponding Author: Chongjiang Cao

E-mail: ccj33@163.com

[1]These authors contributed equally to this work.

1. EXPERIMENTAL SECTION

1.1 Synthesis and characterization

1.1.1 Milling synthesis of UiO-66-NH_2 from the cluster 1 (UiO-66-NH_2 (1))

The UiO-66-NH_2 samples synthesized by this method are uniformly denoted as UiO-66-NH_2 (1). The liquid-assisted grinding (LAG) of UiO-66-NH_2 (1) was performed on a JXFSTPRP-CL-24 high-speed low-temperature grinding instrument at a frequency of 50 Hz, temperature of -30 ℃ and time of 30 min. The reactants (acetate cluster 1:2-Aminoterephthalic acid, molar ratio of 1:6) and 50 μL of anhydrous ethanol were added to a grinding tube (2 mL) with three stainless steel balls (3 mm diameter) was used. The collected yellow powder was centrifuged, washed three times with water and subsequently vacuum dried at 40 ℃.

1.1.2 Milling synthesis of Cel@UiO-66-NH_2 from the cluster 2 (Cel@UiO-66-NH_2 (2))

The Cel@UiO-66-NH_2 composites synthesized by this method are uniformly denoted as Cel@UiO-66-NH_2 (2). The LAG-assisted milling reaction of Cel@UiO-66-NH_2 (2) was performed on a JXFSTPRP-CL-24 high-speed low-temperature grinding instrument at a frequency of 50 Hz, temperature of -30 ℃ and time of 30 min. The reactants (methacrylate cluster 2:2-Aminoterephthalic acid, molar ratio of 1:6), Cel (10 mg) and 50 μL of anhydrous ethanol were added to a grinding tube (2 mL) with three stainless steel balls (3 mm diameter) was used. The collected powder was centrifuged, washed with water and subsequently vacuum dried at 40 ℃.

1.1.3 Synthesis of Cel-on-UiO-66-NH_2 from the cluster 1 (Cel-on-UiO-66-NH_2 (1))

The Cel-on-UiO-66-NH_2 composites synthesized by this method are uniformly

denoted as Cel-on-UiO-66-NH_2 (1). Cel was bound to the surface of the pre-synthesized UIO-66-NH_2 from the methacrylate cluster 2 by stirring, and UiO-66-NH_2 was pre-synthesized according to the method mentioned previously. Initially, 90 mg of UiO-66-NH_2, 10 mg of Cel and 10 mL of H_2O were added to a 50 mL beaker (the mass of UiO-66-NH_2 remains consistent with the mechanochemical encapsulation method described above). Then, the mixture was stirred at room temperature with a magnetic stirrer, at 300 rpm for 30 min. The collected powder was centrifuged, washed with water and subsequently vacuum dried at 40 ℃.

1.2 Activity of Cel

The cellulase activity was determined by the carboxymethyl cellulose assay according to the formulation of Mubarak et al. with the following modifications [1]. The Cel mass was kept consistent for each experiment, and the enzyme@MOF materials containing the same Cel mass was dispersed into 4 mL of citrate buffer (pH 4.8, 50 mM) containing 1% carboxymethyl cellulose. The samples were then subjected to an incubator shaker at 50 ℃, 120 rpm for 30 min. Then, 0.8 mL of NaOH (0.2 M) was added to the centrifuge tube to terminate the hydrolysis reaction. The above reaction solution was centrifuged at 10 000 rpm for 10 min, 1 mL of supernatant was taken, 1 mL of DNS reagent was quickly added, mixed well, while placed in a boiling water bath, heated for 10 min, removed and cooled to room temperature, and fixed to 10 mL with water, and the final concentration of glucose was calculated by measuring the absorbance at a wavelength of 540 nm using a Multiskan FC microplate reader (Thermo Fisher Scientific). For denature reagent treatment, denaturant (urea or 3-AT) was added

to the solution before the reaction to contain a final concentration of 0.5 M urea or 0.01 M 3-AT, and the samples were subsequently reacted in an incubator shaker [2].

1.3 Hydrolysis (in situ saccharification) of microcrystalline cellulose

In a conical flask, 0.1 g of microcrystalline cellulose, 5 mL of citrate buffer (pH 4.8, 50 mM) and 10 mg of cellulase or enzyme@MOF material containing the same quality of cellulase were added, and then the samples were put into a thermostatic oscillator at 50 ℃ and 120 rpm to oscillate for 30 min for 5 h. The rest of the operation was as above.

1.4 BCA assay

In this study, the BCA protein assay kit was utilized as a standard method for protein concentration determination to determine the protein loading of the enzyme@MOF complexes obtained by different synthesis methods [3]. BCA protein assay kit was purchased from Beyotime. The standard operating protocol provided by the supplier was followed.

1.5 SDS–PAGE analysis of Cel@UiO-66-NH_2

To ensure that enzyme has been encapsulated into UiO-66-NH_2, 90.0 mg of Cel@UiO-66-NH_2 was dissolved in 2.0 mL of 0.3 M NaOH and sonicated for 30 min. After complete dissolution of the powder, it was concentrated by centrifugation for a few minutes. Then, 100.0 μL of the supernatant was mixed with 25 μL of loading buffer (125 mM Tris-HCl (pH 6.8), 2% SDS, 0.1% bromophenol blue, 10% glycerol and 10% β-mercaptoethanol) and heated in water at 100 °C for 10 min. The mixture was then loaded on a gel and electrophoresed on SDS-PAGE (10% acrylamide separating gel and

5% acrylamide stacking gel). After completion of the electrophoresis , a rapid staining with Commassie Blue was performed according to the instruction [4].

1.6 Reusability and stability test of Cel@UiO-66-NH_2

The hydrolytic stability of immobilized Cel was assessed using ten consecutive hydrolysis reactions. After each reaction, immobilized Cel was collected by centrifugation (10 000 rpm, 10 min), washed twice with citrate buffer (pH 4.8, 50 mM) to remove residual substrate and product, and dried under vacuum at 40 ℃. The dried samples were reweighed and used for the next cycle.

The enzymatic activities of Cel and Cel@UiO-66-NH_2 were examined at pH 3.0~7.0 and temperature 30~80 ℃.

1.7 Enzyme active site pocket and spatial structure analysis activity pocket analysis

1.6.1 Enzyme activity pocket analysis

Crystal structure data of Endoglucanase (EC:3.2.1.4), Exoglucanase (EC:3.2.1.91) and Beta-glucosidase (EC:3.2.1.21) were obtained from the Protein Data Bank website Uniprot (http://wwwuniprot.org/) (PDB: 2BOG, 2YOK and 6JXG), and the identified active site amino acid based binding pocket grid of the above three enzymes were analyzed using the molecular operating environment (MOE) software to map their activity pockets at a distance of 5 A° around their substrates.

1.6.2 Enzyme spatial structure analysis

After importing the crystal structure data of Endoglucanase (EC:3.2.1.4), Exoglucanase (EC:3.2.1.91) and Beta-glucosidase (EC:3.2.1.21) (PDB: 2BOG, 2YOK

and 6JXG) into Pymol, respectively, use the The "Draw Protein Dimensions" function displays the length, width, and height of the protein and outputs its spatial size separately.

1.8 Biocompatibility

1.8.1 Cell lines and culture

HaCaT cells were cultured in MEM medium supplemented with 10% fetal bovine serum and 1% (vol/vol) penicillin-streptomycin.

1.8.2 Cell viability

Referring to the method of Liu et al [5], with some modifications, the CCK8 assay was used to assess cell viability. HacaT cells were treated with trypsin and inoculated into 96-deepwell plates at a density of 5×10^3 cells/well in 100 μL MEM medium. The medium in each well was discarded after 24 hours of incubation at 37°C and 5% CO_2. Then, 100 μL MEM medium amended with 0, 100, 200, 300, 400 and 500 μg/mL UiO-66-NH_2 (1) or UiO-66-NH_2 (2) was added to each well and incubated for 24 hours. Every 6 wells were treated with a specific dose, and zero dosage was set as the control for all in vitro experiments, the medium in the wells was replaced with 10% CCK8 solution and the cells were incubated at 37°C for 1 hour. Cell viability was then assessed by measuring the optical density of each well at 450 nm using a microplate reader (Multiskan FC, Thermo Fisher, USA). All data were corrected for the cell-free control and the level of cell inhibition was calculated using the following equation.

$$\text{Cell viability (\%)} = \frac{\text{OD}_{\text{treated}}}{\text{OD}_{\text{control}}} \times 100\% \quad (2)$$

1.9 Fluorescein-Tagged Enzyme

The protocol is based on a previously reported procedure [6] with slight modifications. Dissolve 50 mg of the enzyme in 2.5 mL of saline as a stock solution of the enzyme. Subsequently, fluorescein-5-isothiocyanate (FITC) solution was prepared using carbonate-bicarbonate buffer (pH 9.6, 50 mM) with a FITC concentration of 10.0 mg/mL. the enzyme stock solution was mixed with the FITC solution and stirred for 30 min, and the resulting solution was dialyzed using a dialysis bag (MW: 3500) and washed with citrate buffer (pH 4.8. 50 mM) for washing. The purified FITC-Cel (FCel) solution was then lyophilized and stored at 4°C until further use.

1.10 Extraction of *N. aurantialba* polysaccharides

1.10.1 Enzyme- assisted hot water extraction

0.2 g of dried *N. aurantialba* fruiting bodies powder and 10 mg of immobilized cellulase were mixed with 40 mL of distilled water and extracted for 3 hours at 70 °C.The immobilized cellulase was recovered by centrifugation at 10,000 rpm for 10 min. The supernatant was collected by centrifugation at 10,000 rpm for 10 min and precipitated with ethanol at a final concentration of 75 % at 4 °C. Collect the precipitate by centrifugation. The crude polysaccharide was obtained by dialysis (35,000 Da) and freeze-drying.[7, 8]

1.10.2 Chemical analysis of N. aurantialba polysaccharides

Carbohydrate content in *N. aurantialba* polysaccharides was determined by phenol-sulfuric acid method.[8]

2. ADDITIONAL DATA

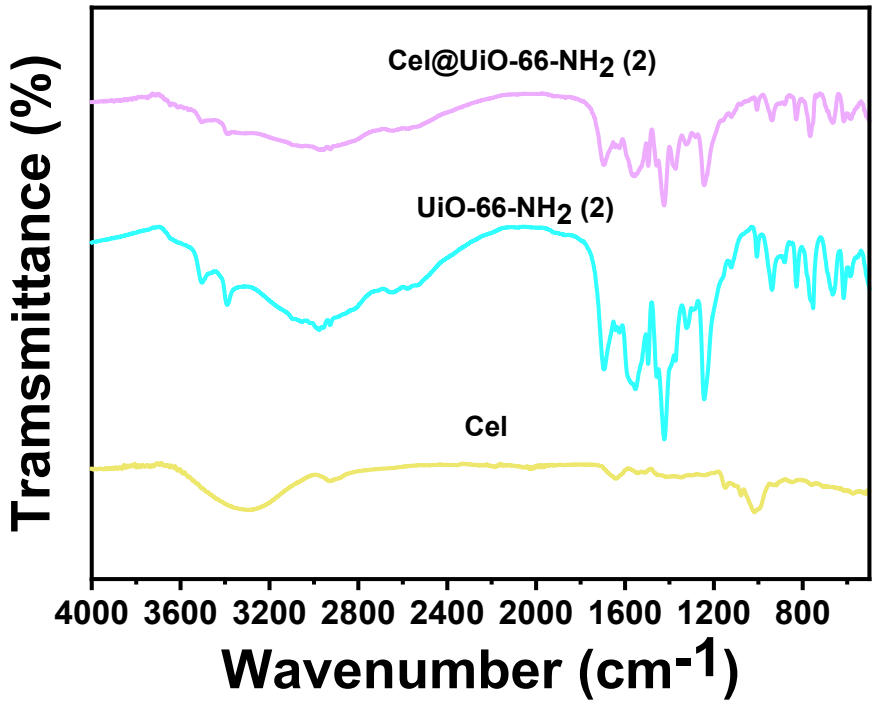

Figure S1. FT-IR of Cel@UiO-66-NH_2 (2), UiO-66-NH_2 (2) and Cel.

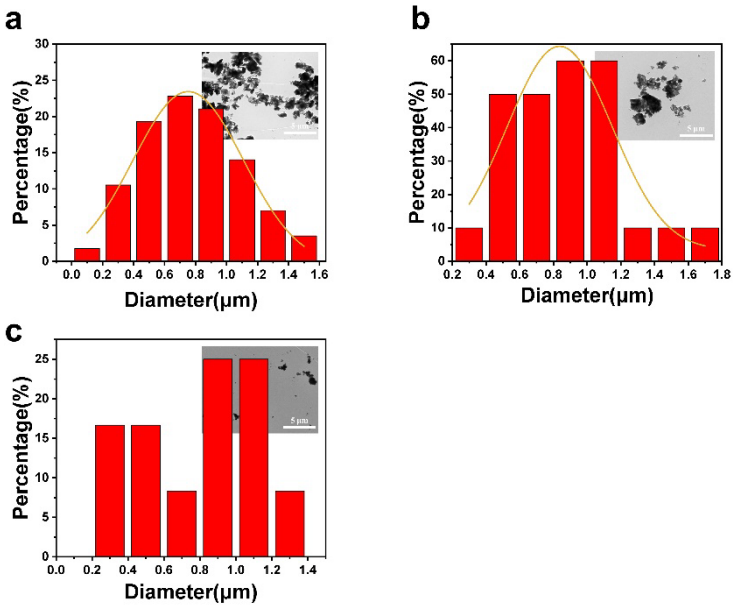

Fig. S2. Particle size distribution of (a) UiO-66-NH_2 (1), (b-c) Cel@UiO-66-NH_2 (1) and (d) Cel-on-UiO-66-NH_2 (1)

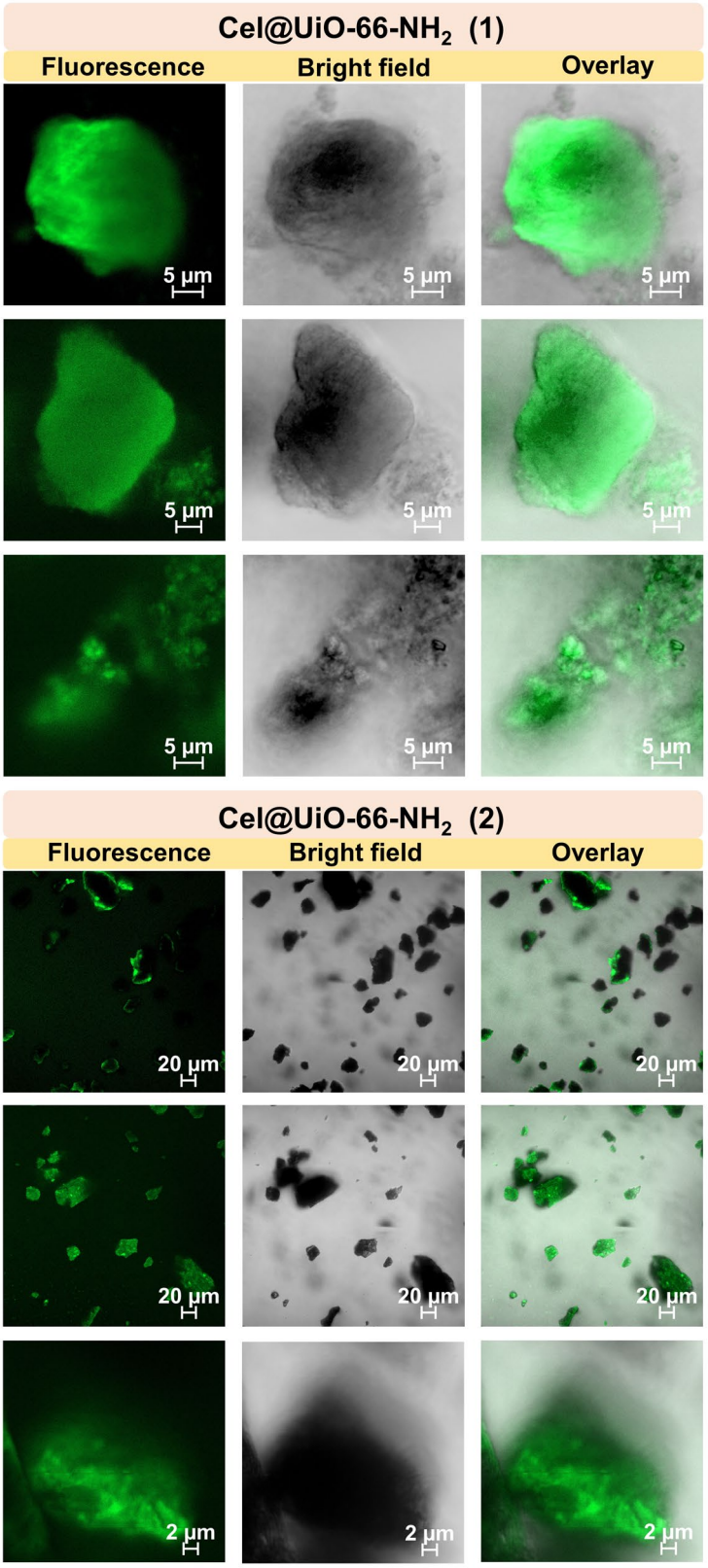

Figure S3. CLSM images of Cel@UiO-66-NH_2 (1) and Cel@UiO-66-NH_2.

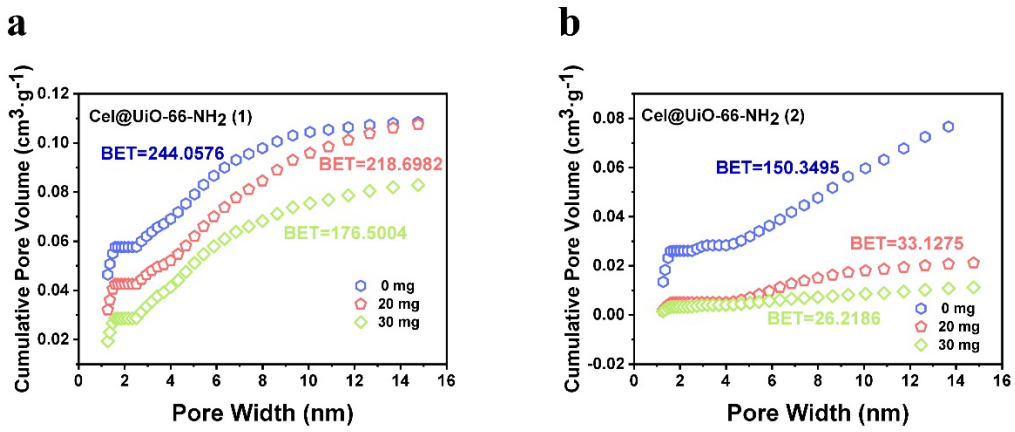

Figure S4. Cumulative pore volume of (a) Cel@UiO-66-NH_2 (1) and (b) Cel@UiO-66-NH_2 (2) with different enzyme loadings (0, 20, and 30 mg).

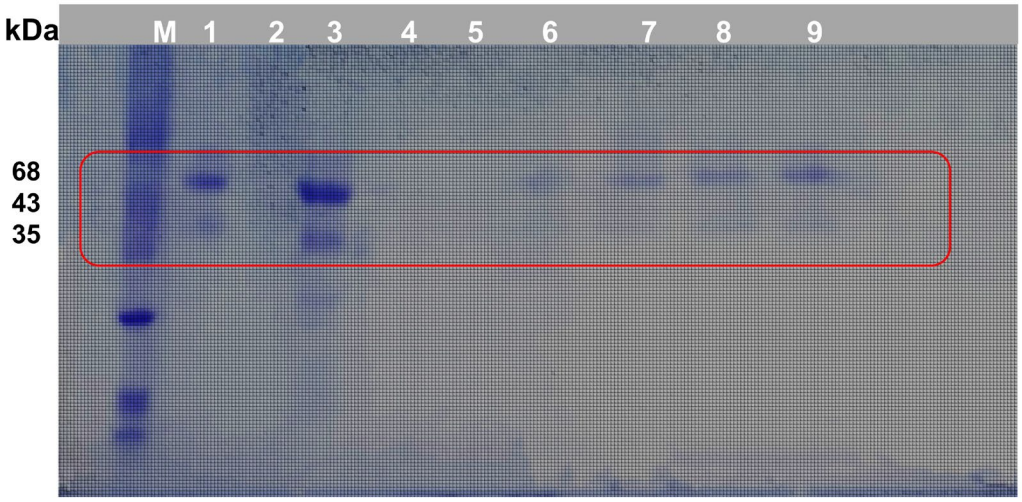

Figure S5. SDS−PAGE gel of M, protein marker; 1, Cel; 2, Washed Cel@UiO-66-NH_2 (1); 3, Washed Cel@UiO-66-NH_2 (2); 4, Washed Cel-on-UiO-66-NH_2 (1); 5, Washed Cel-on-UiO-66-NH_2 (2); 6, Cel@UiO-66-NH_2 (1); 7, Cel@UiO-66-NH_2 (2); 8, Cel-on-UiO-66-NH_2 (1); 9, Cel-on-UiO-66-NH_2 (2).

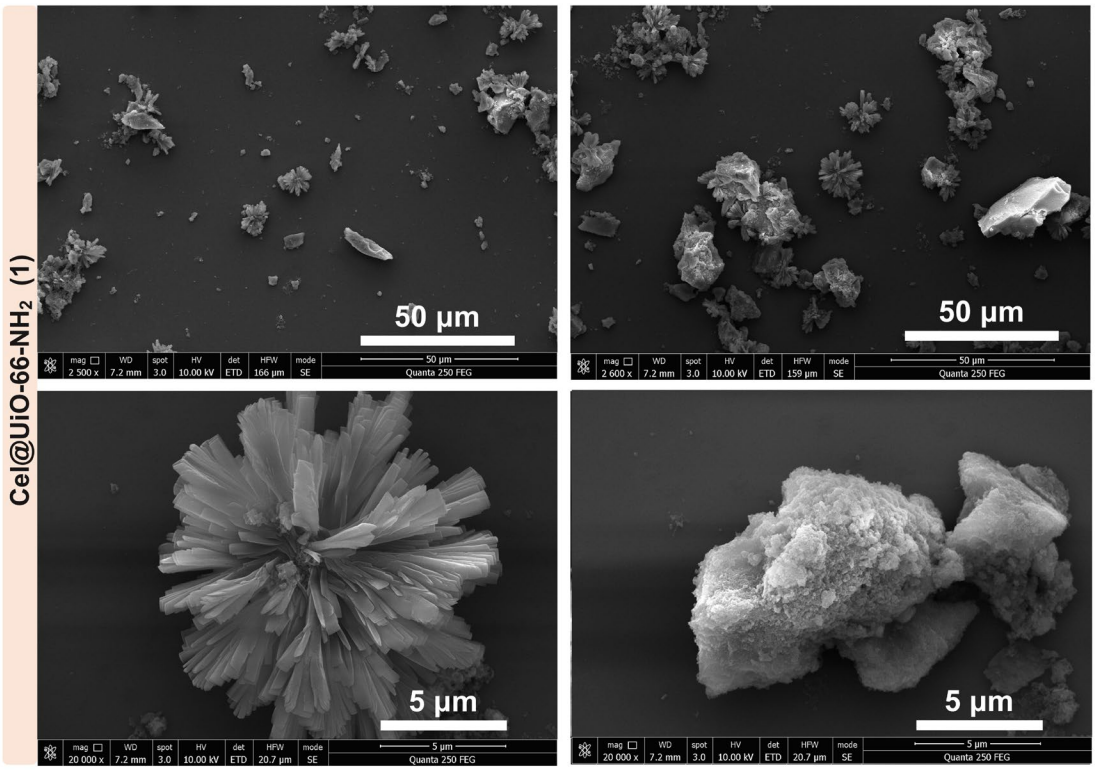

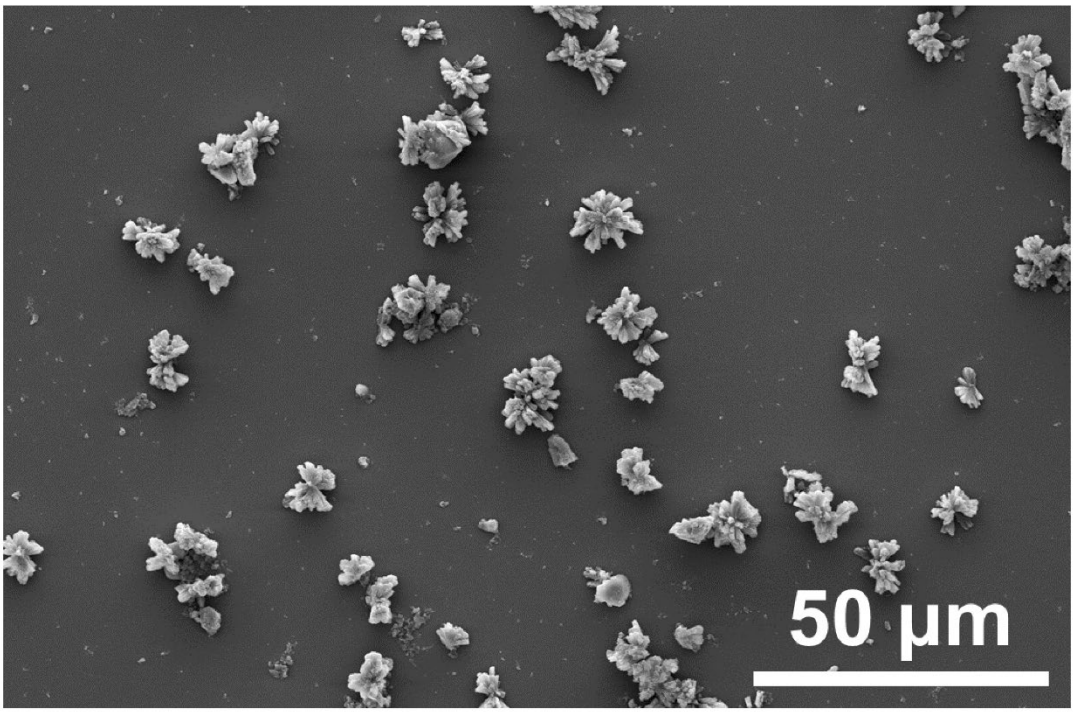

Figure S6. SEM images of Cel@UiO-66-NH_2 (1).

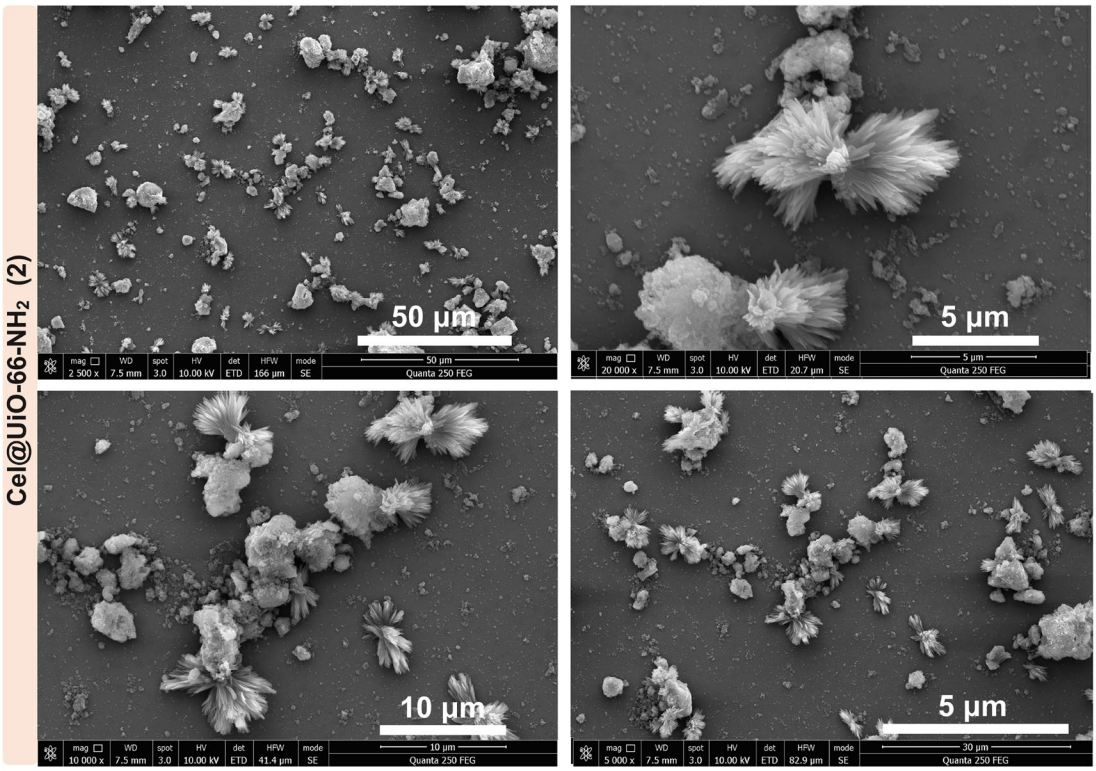

Figure S7. SEM images of Cel@UiO-66-NH_2 (2).

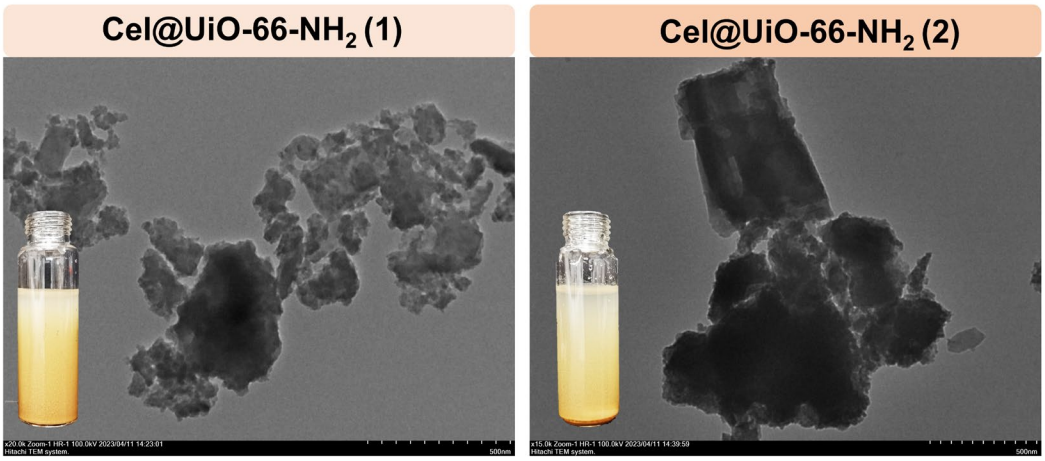

Figure S8. TEM and optical images of Cel@UiO-66-NH_2 (1) and Cel@UiO-66-NH_2 (2) solution.

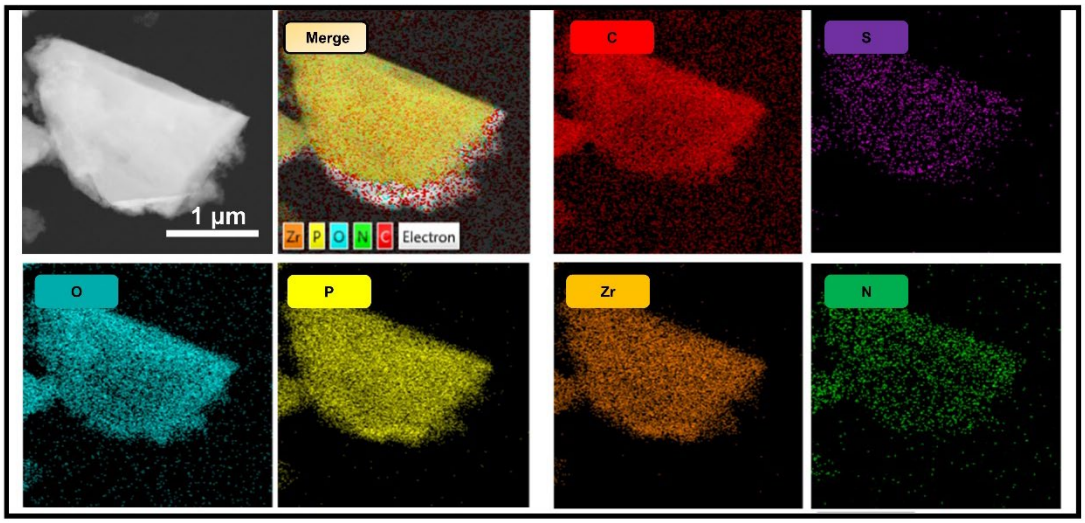

Figure S9. EDX images of Cel@UiO-66-NH_2 (1).

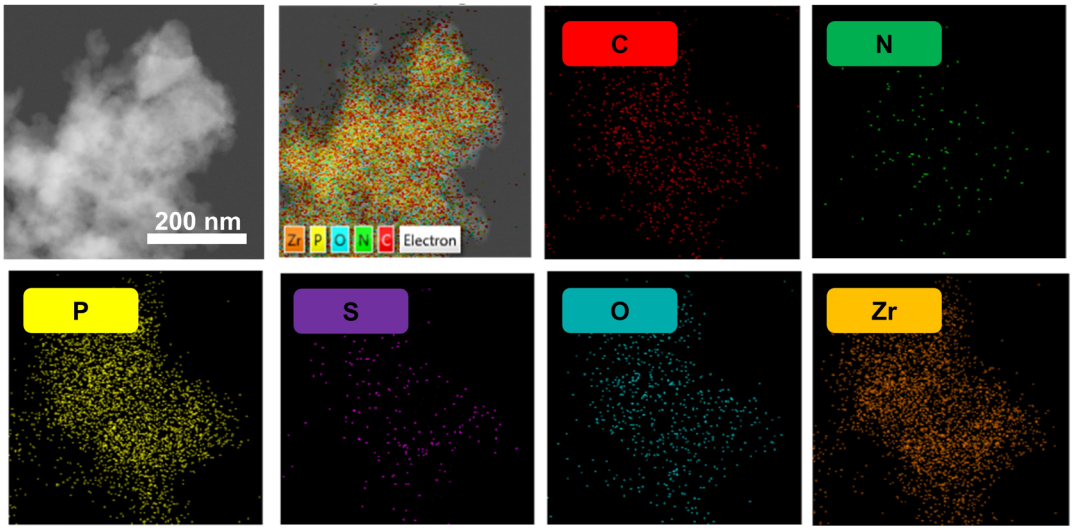

Figure S10. EDX images of Cel@UiO-66-NH_2 (2).

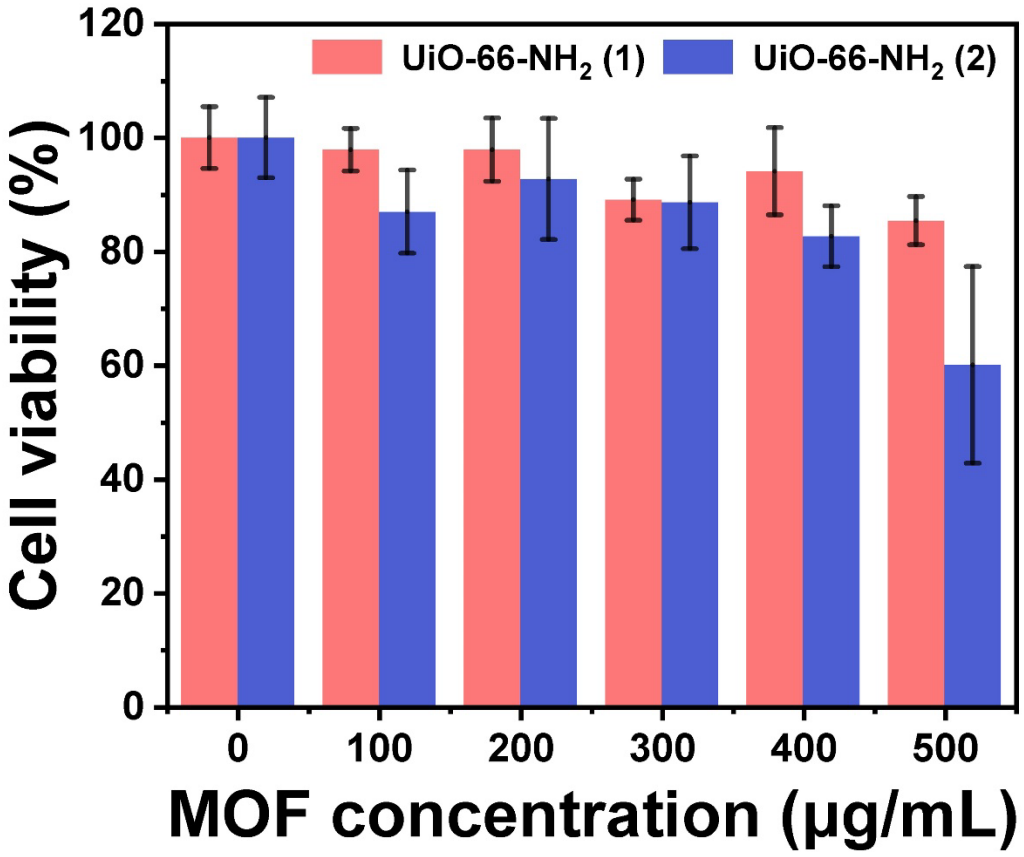

Figure S11. Cytotoxicity test of UiO-66-NH_2 (1) and UiO-66-NH_2 (2) on HaCaT cells. The error bar represents the standard deviation (n = 3).

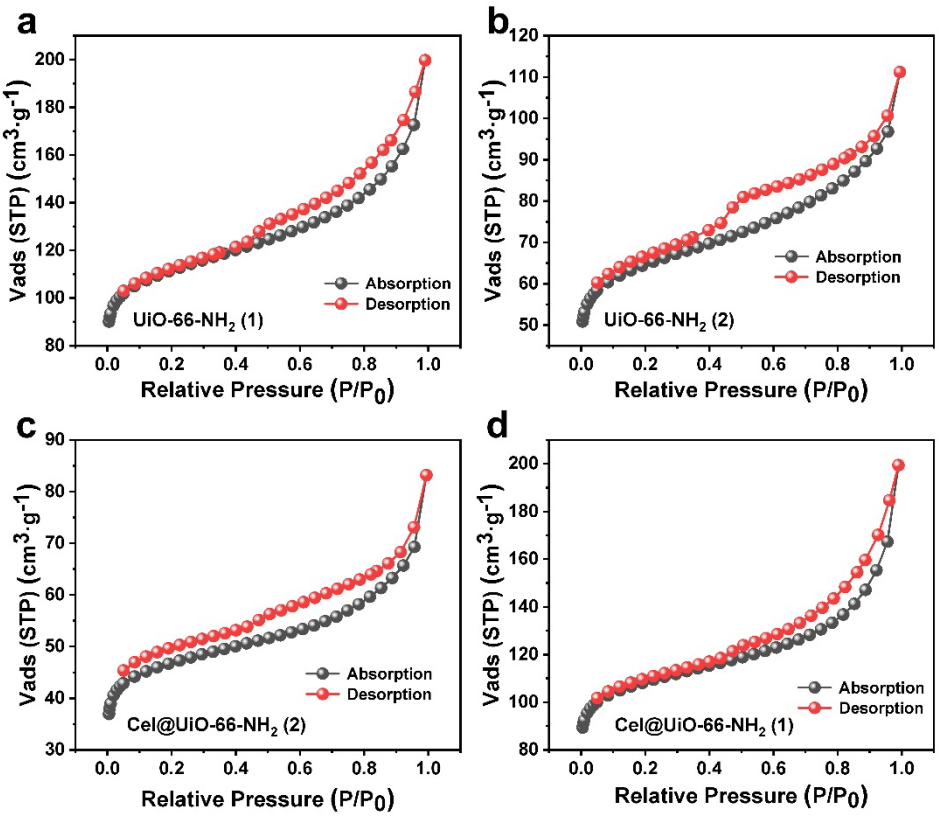

Figure S12. Characterization of the hierarchical pore structure of UiO-66-NH_2 (1), Cel@UiO-66-NH_2 (1), UiO-66-NH_2 (2), and Cel@UiO-66-NH_2 (2). (a-d) N_2 adsorption-desorption isotherms.

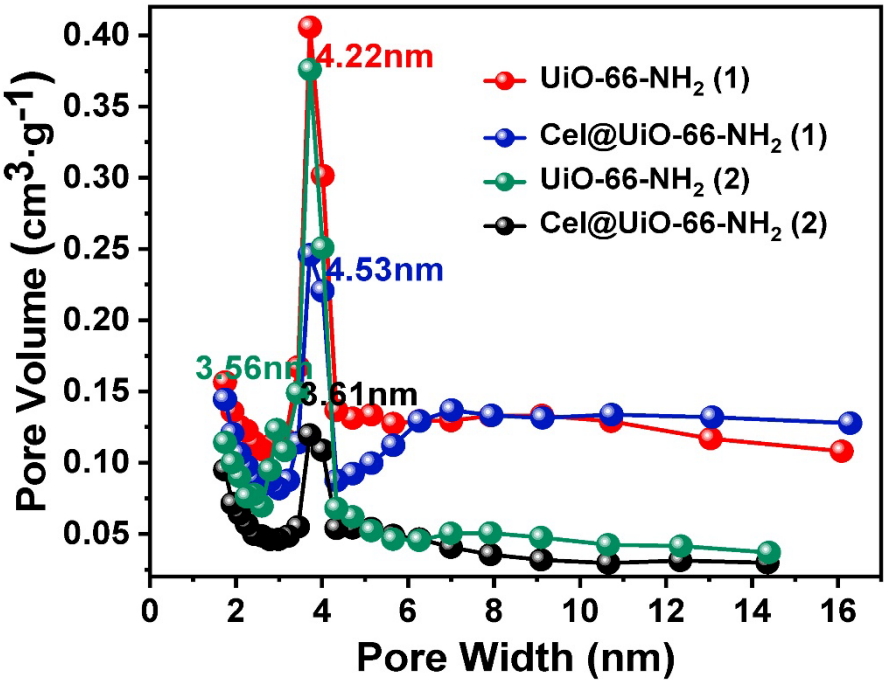

Figure S13. Pore size distributions of UiO-66-NH_2 (1), Cel@UiO-66-NH_2 (1), UiO-66-NH_2 (2), and Cel@UiO-66-NH_2 (2)

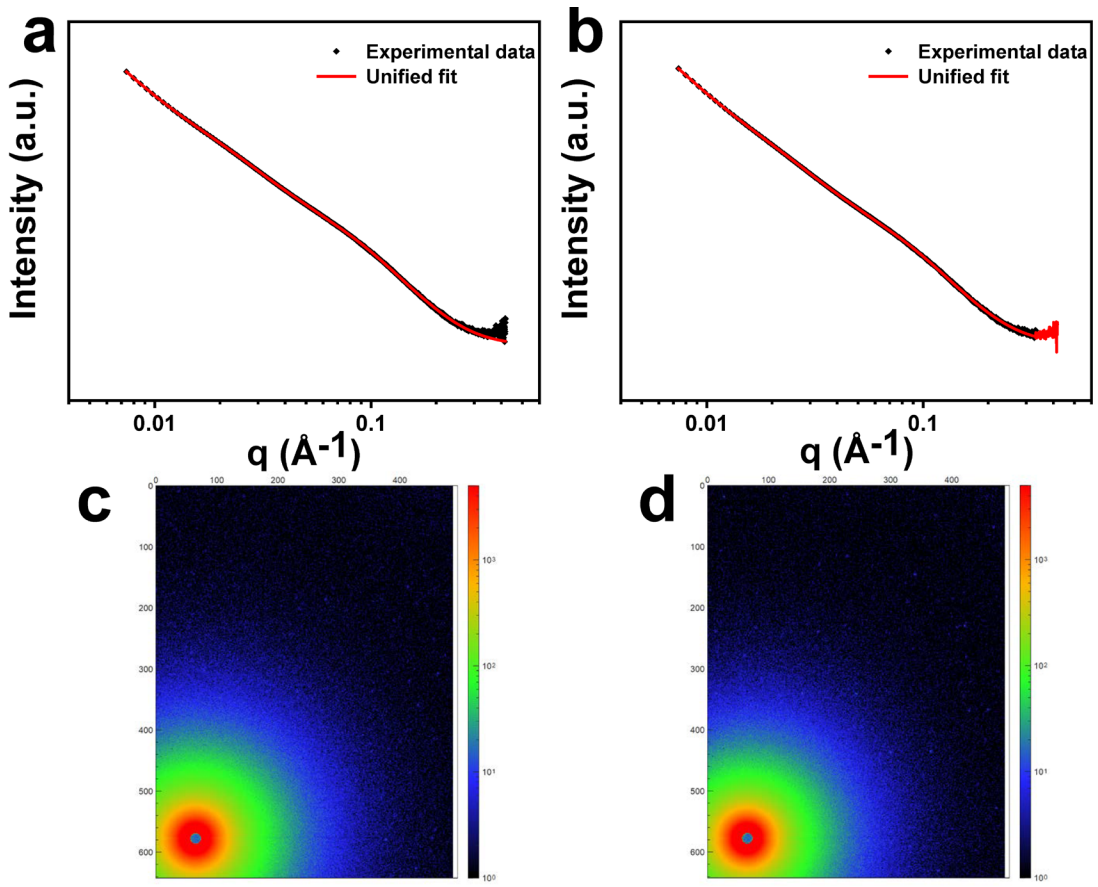

Figure S14. Representative Guinier approximations (red) for raw SAXS spectra (black) of (a) UiO-66-NH_2 (1) and (b) Cel@UiO-66-NH_2 (1) at room temperature (Q: 0.0074 $Å^{-1}$ - 0.4 $Å^{-1}$); Two-dimensional (2D) SAXS scattering patterns of (c) UiO-66-NH_2 (1) and (d) Cel@UiO-66-NH_2 (1).

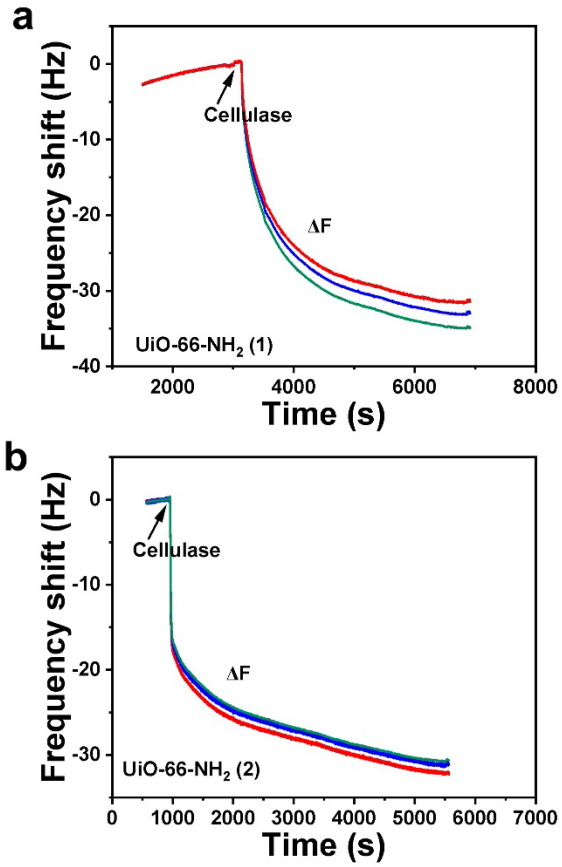

Figure S15. Frequency shift (Δf) profiles showing adsorption and desorption behavior of Cel with UiO-66-NH_2 (1) (a) or UiO-66-NH_2 (2) (b).

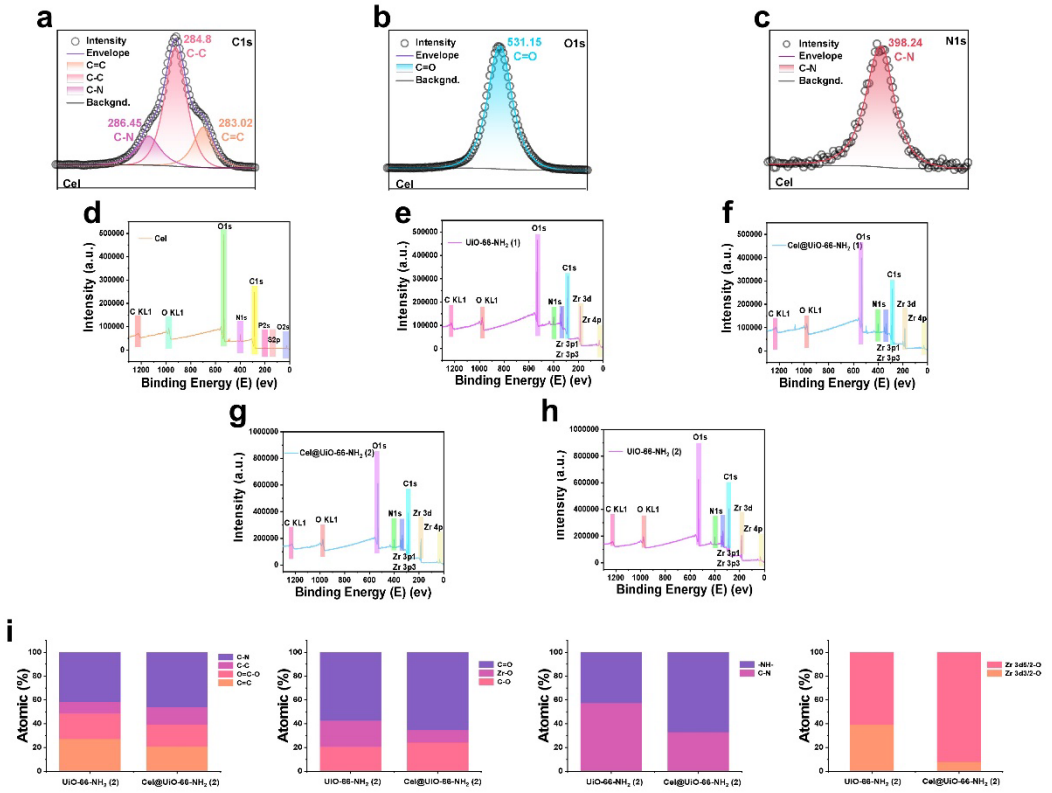

Figure S16. XPS analysis reveals chemical bonding changes. (a) C 1s high-resolution spectra, (b) O 1s high-resolution spectra, (c) N 1s high-resolution spectra of Cel; (d-h) XPS survey spectra; (i) Atomic percentages of UiO-66-NH_2 (2), and Cel@UiO-66-NH_2 (2) on the basis of the XPS spectra.

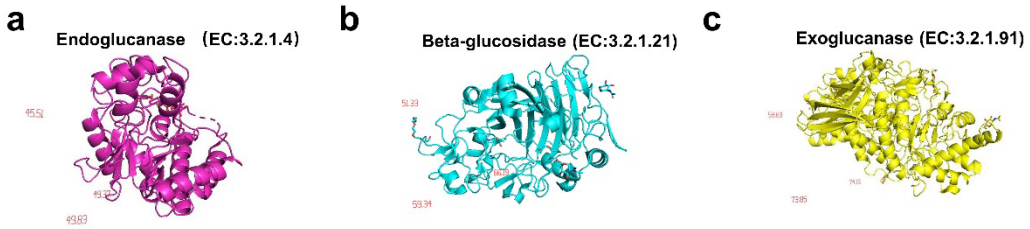

Figure S17. (a-c) Spatial structure of Cel (Endoglucanase (EC:3.2.1.4), Beta-glucosidase (EC:3.2.1.21), and Exoglucanase (EC:3.2.1.91)).

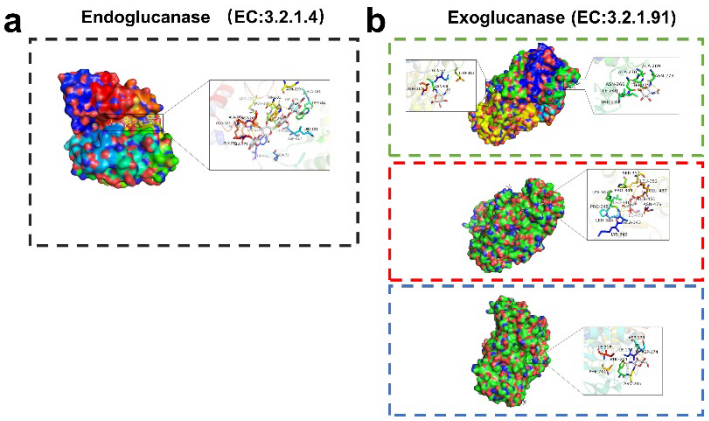

Figure S18. (a-b) Active site pocket and the amino acid residues of Cel interacting with the substrate.

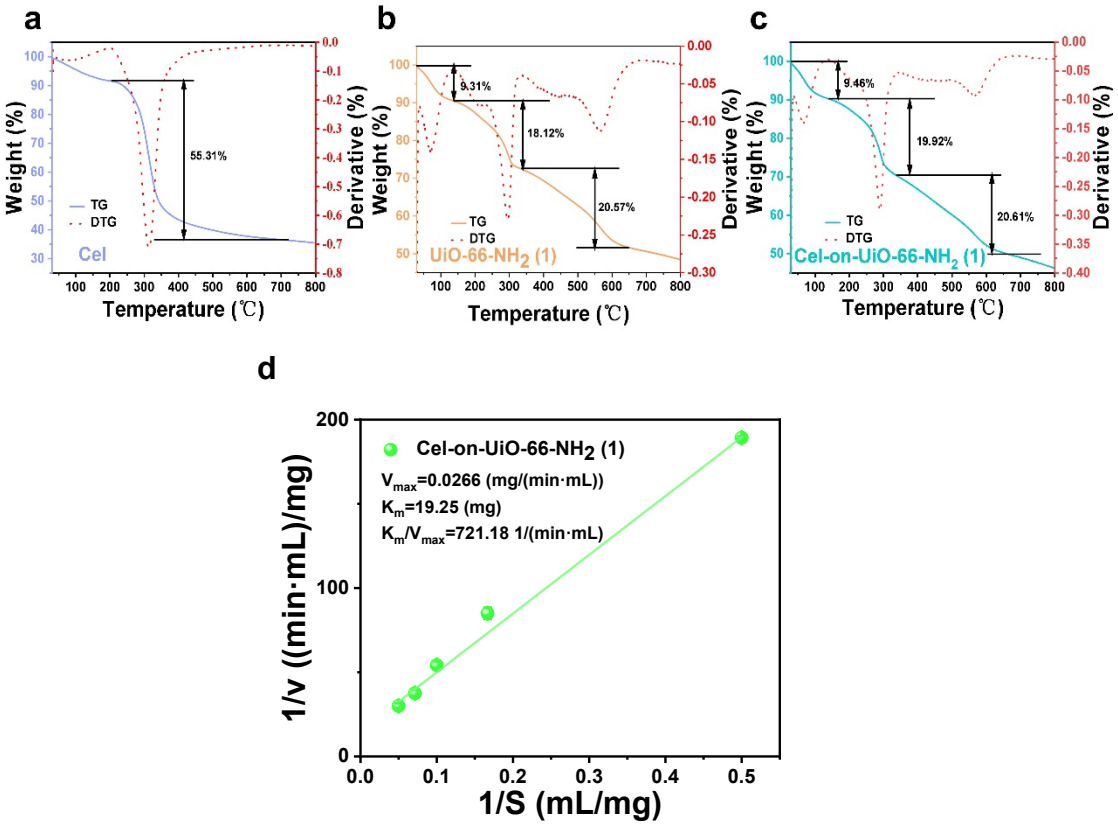

Figure S19. TGA curves of (a) Cel, (b) UiO -66-NH_2 (1) and (c) Cel-on-UiO -66-NH_2 (1); (d) Calculated catalytic kinetic parameters of Cel-on-UiO-66-NH_2 (1).

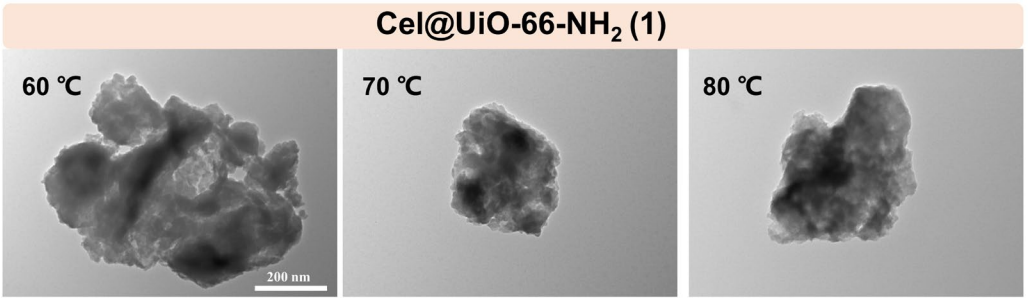

Figure S20. TEM images of Cel@UiO-66-NH_2 (1) after different temperatures (60 °C, 70 °C and 80 °C) incubation.

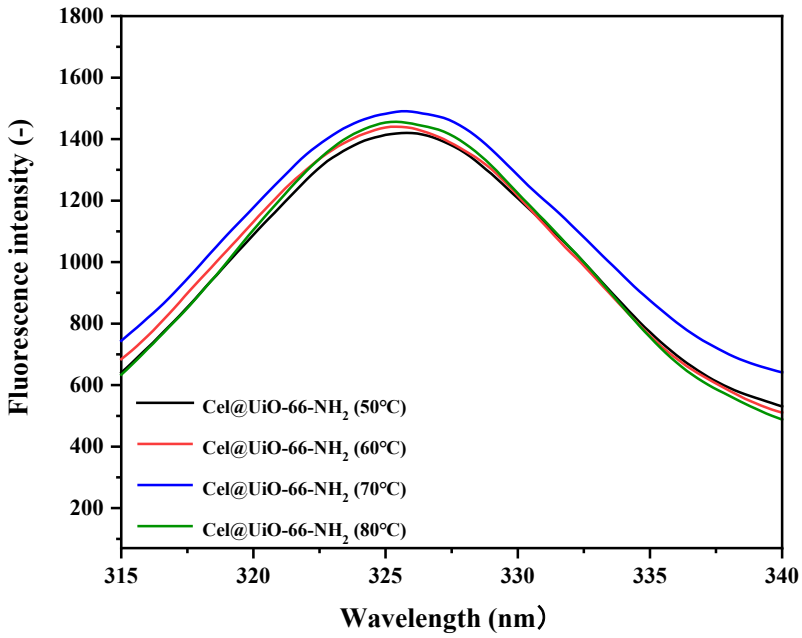

Figure S21. Fluorescence spectra of Cel@UiO-66-NH_2 (1) after different temperatures (50℃, 60 °C, 70 °C and 80 °C) incubation.

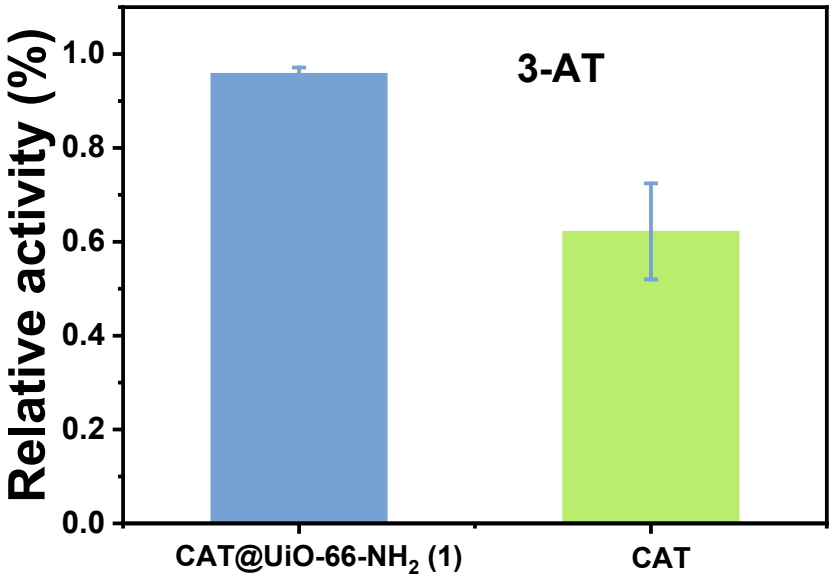

Figure S22. Relative activity after 0.5 h 3-AT treatment (untreated = 100%).

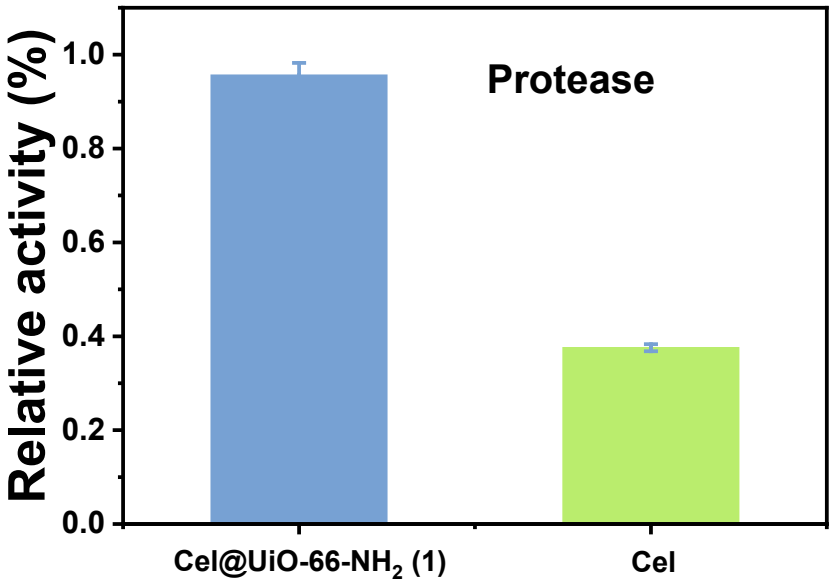

Figure S23. Relative activity after 0.5 h proteinase K treatment (untreated = 100%).

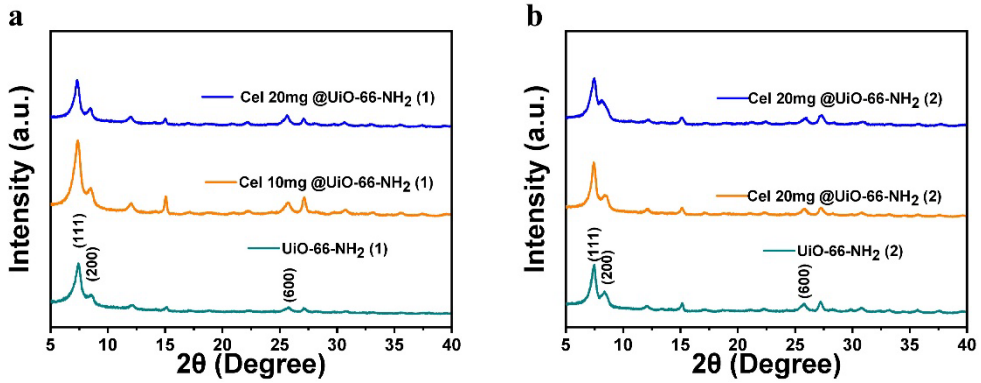

Figure S24. XRD patterns of Cel@UiO-66-NH2 (1) and Cel@UiO-66-NH2 (2) at different time points.

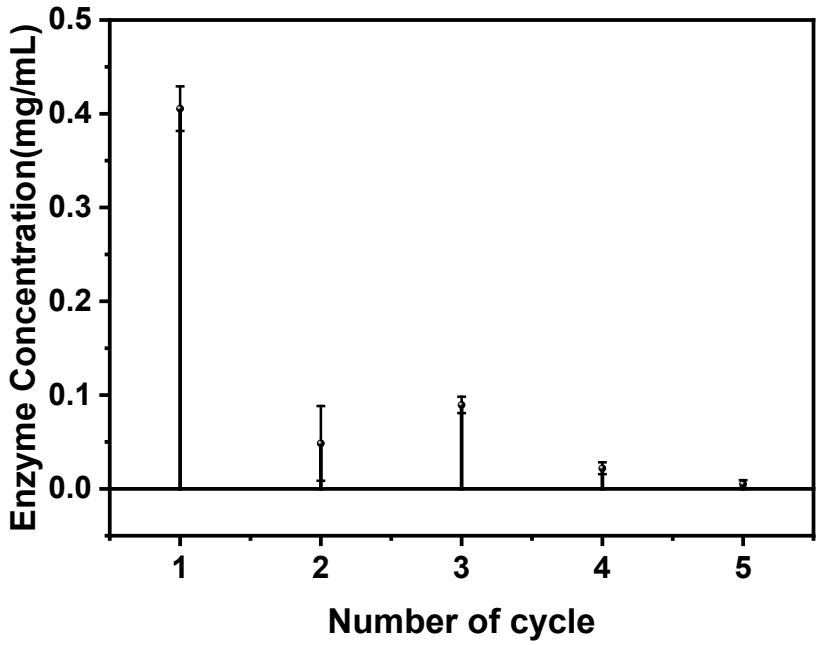

Figure S25. The Cel@UiO-66-NH_2 (1) was subjected to five catalytic cycles, with enzyme leaching in the supernatant quantified after each cycle using the BCA assay kit

REFERENCES

1 N. Mubarak, J. Wong, K. Tan, J. Sahu, E. Abdullah, N. Jayakumar and P. Ganesan, *J. Mol. Catal. B: Enzym.*, 2014, **107**, 124-131.

2 F.-S. Liao, W.-S. Lo, Y.-S. Hsu, C.-C. Wu, S.-C. Wang, F.-K. Shieh, J. V. Morabito, L.-Y. Chou, K. C.-W. Wu and C.-K. Tsung, *J. Am. Chem. Soc.*, 2017, **139**, 6530-6533.

3 J. Liang, M. Y. Bin Zulkifli, J. Yong, Z. Du, Z. Ao, A. Rawal, J. A. Scott, J. R. Harmer, J. Wang and K. Liang, *J. Am. Chem. Soc.*, 2022, **144**, 17865-17875.

4 L. Amagliani, J. O'Regan, A. L. Kelly and J. A. O'Mahony, *J. Food Compos. Anal.*, 2017, **59**, 18-26.

5 D. Liu, Y. Yang, Q. Liu and J. Wang, *Med. Oncol.*, 2011, **28**, 105-111.

6 W. Liang, H. Xu, F. Carraro, N. K. Maddigan, Q. Li, S. G. Bell, D. M. Huang, A. Tarzia, M. B. Solomon, H. Amenitsch, L. Vaccari, C. J. Sumby, P. Falcaro and C. J. Doonan, *J. Am. Chem. Soc.*, 2019, **141**, 2348-2355.

7 L. Sun, J. Jiang, T. Jing, D. Hu, J. Zhu, Y. Zeng, Y. Pang, D. Huang, S. Cheng and C. Cao, *Carbohydr. Polym.*, 2023, **318**, 121124.

8 Y. Sun, Q. Nie, S. Zhang, H. He, S. Zuo, C. Chen, J. Yang, H. Chen, J. Hu, S. Li, J. Cheng, B. Zhang, Z. Zheng, S. Pan, P. Huang, L. Lian and S. Nie, *Nat. Commun.*, 2023, **14**, 7740.